Expression and significance analyses of microRNAs in colorectal cancer

JING ZHANG[1*], LIWEI SUN[2*], CHANGXIU YAN[2*], HONGGANG RAN[3], KAIYONG QU[3], ZHIJIAN CHEN[3], ARGEN BAHET[3], CHENXI WANG[3], XIN CAI[3], GUOHONG ZHUANG[2] and ZEYANG LIN[4]

[1]Department of Laboratory Medicine, Fujian Key Clinical Specialty of Laboratory Medicine, Women and Children's Hospital, School of Medicine, Xiamen University, Xiamen, Fujian 361000, P.R. China; [2]Organ Transplantation Institute of Xiamen University, Fujian Provincial Key Laboratory of Organ and Tissue Regeneration, School of Medicine, Xiamen University, Xiamen, Fujian 361000, P.R. China; [3]School of Medicine, Xiamen University, Xiamen, Fujian 361000, P.R. China; [4]Department of Pathology, Zhongshan Hospital of Xiamen University, School of Medicine, Xiamen University, Xiamen, Fujian 361000, P.R. China

Received June 4, 2025; Accepted January 8, 2026

DOI: 10.3892/mco.2026.2929

Abstract. MicroRNAs (miRNAs or miRs) serve as potential diagnostic and prognostic markers or therapeutic targets. However, their roles in the pathogenesis of colorectal cancer (CRC) is not fully understood. The aim of the present study was to investigate the expression levels and functions of miR-205, miR-376c, and miR-539 in CRC development and prognosis. Multiple GEO databases were used to explore miRNA expression levels and associations in CRC cancer and adjacent/normal tissues. In addition, the associations between the expression of the miRNAs and the clinicopathological features of CRC were analyzed. The clinical data and specimens of 25 patients with CRC were collected, detected and analyzed. Combining bioinformatics analysis and databases, the relationship between the three miRNAs and CRC progression and prognosis was explored. In the GSE41655 dataset, miR-376c, miR-539, and miR-205 were all downregulated in tumor tissues, with miRNA-376c exhibiting the most pronounced downregulation. MiR-376c was closely associated with CRC liver metastasis, especially in the synchronous metastasis condition. Additionally, in the miRDB database, an analysis of the overlapping predicted target genes for miR-205, miR-376c, and miR-539 revealed that these three miRNAs share 53 common predicted target genes. Not only did miR-539 and miR-205 significantly differ according to tumor stage and lymph node metastasis, but also their upregulation was significant in tumor advanced stage and lymph node metastasis according to logistic regression in collected cancer tissues. Furthermore, miR-205 was significantly upregulated in tumor differentiation according to logistic regression. In conclusion, miR-205, miR-376c, and miR-539 were revealed to be involved in the development and prognosis of CRC and may be potential targets for CRC therapy.

Correspondence to: Dr Guohong Zhuang, Organ Transplantation Institute of Xiamen University, Fujian Provincial Key Laboratory of Organ and Tissue Regeneration, School of Medicine, Xiamen University, 42 Siming South Road, Haibin Street, Xiamen, Fujian 361000, P.R. China
E-mail: zhgh@xmu.edu.cn

Dr Zeyang Lin, Department of Pathology, Zhongshan Hospital of Xiamen University, School of Medicine, Xiamen University, 201 Hubin South Road, Kaiyuan Street, Xiamen, Fujian 361000, P.R. China
E-mail: zeyanglin@xmu.edu.cn

*Contributed equally

Key words: colorectal cancer, miR-205, miR-376c, miR-539

Introduction

Colorectal cancer (CRC) is one of the most common types of malignant tumors of the digestive tract and ranks third among new estimated cases and deaths among men and women globally. At first, most patients with CRC in stages I and II undergo only partial or total colectomy, and then approximately two-thirds with stage III undergo chemotherapy to reduce the risk of recurrence. Ultimately, chemotherapy is the main treatment of patients with CRC in stage IV. With ~2 million new cases and 1 million deaths worldwide in 2020, CRC ranks as the third and second most frequent cause of cancer incidence and mortality, respectively (1). Based on research, targeted drugs can prevent the growth of cancer cells through the action of specific molecular targets necessary for cancer development and tumor growth and can also be used to treat metastatic CRC. Activation or inactivation of oncogenes and tumor suppressor genes are classic markers of these tumors, and the relevant mechanisms have been the core target of cancer research (2). Studying key molecular mechanisms required for growth and metastasis will greatly assist in the advancement of targeted therapies to improve the condition and prognosis of patients with CRC (3).

MicroRNAs (miRNAs or miRs) are a class of evolutionarily conserved small non-coding RNAs, which are 17-25 nucleotides in length. They bind to the 3'-untranslated regions (UTRs) of their target mRNAs, affecting mRNA stability or inhibiting its translation. miRNAs regulate gene expression

at the post-transcriptional level (4). Abnormalities in miRNA expression are linked to diverse biological changes, including cell proliferation, apoptosis, differentiation, and tumorigenesis (5). Numerous studies have shown that miRNAs are closely related to the occurrence, development, and progression of tumors (6,7). Therefore, they may serve as new and promising therapeutic targets.

Research has found that miR-539 inhibits human CRC progression by targeting RUNX2 (8). miR-205 can be upregulated or downregulated in human CRC, and p53 has been shown to regulate CRC metastasis by inhibiting SQLE expression by inducing miR-205 (9). Cisplatin was demonstrated to inhibit the proliferation of Saos-2 cells by upregulating miR-376c and downregulating TGFA expression (10). miR-539 is located on human chromosome 4q32.31 and it is reportedly downregulated in a variety of human cancers, including nasopharyngeal, prostate, and thyroid cancers. Furthermore, miR-539 has been shown to be a tumor suppressor in human malignancies (11). Combining the present research and reviewing relevant literature, miR-205, miR-376c, and miR-539 (which are related to tumor necrosis factor-α induced protein 8) were selected as research targets, and their roles in the development and progression of CRC were explored. The purpose of the presen study was to analyze the expression patterns of these three miRNAs in CRC, determine their clinical significance, and combine their expression characteristics in CRC to delineate their roles in the development of CRC and provide a novel therapeutic target for prognosis. The research protocol is shown in a schematic flowchart (Fig. 1).

Materials and methods

Bioinformatics analyses. MiRNA microarray data of solitary CRC were obtained from the Gene Expression Omnibus (GEO) database (https://www.ncbi.nlm.nih.gov/geo/) and the University of Alabama at Birmingham CANcer data analysis Portal (UALCAN) (https://ualcan.path.uab.edu/analysis-mir.html). The GSE41655 and GSE81581 datasets were used to investigate the expression of miR-205, miR-376c, and miR-539 in CRC (12,13). miRNA sequences and predicted target gene data were primarily sourced from miRDB (https://mirdb.org/) and miRBase (https://www.mirbase.org/).

Relevant miRNA expression data were downloaded from the GEO database based on the GSEE41655 and GSE81581 datasets (13). The downloaded raw data were preliminarily processed and standardized in RStudio 2025.5.1.513 using the Bioconductor 3.18 package (14). Statistical analysis was performed using GraphPad Prism 10.6.1 software (Dotmatics). After performing a normality test on the expressed data, the Kruskal-Wallis test was selected for nonparametric analysis. Subsequently, Dunn's post hoc pairwise multiple comparisons were conducted for groups showing significant differences to obtain the results. The significance level was then set and Bonferroni correction was applied for multiple comparison adjustments. Concurrently, Spearman's ρ correlation analysis was employed to perform pairwise correlation analyses on the acquired data, generating correlation heatmaps. Bonferroni correction was applied to each correlation test.

The Cancer Genome Atlas (TCGA) analysis portal in UALCAN was selected, the colorectal adenocarcinoma (COAD) dataset was chosen, and the differences in the expression between cancerous and normal tissues were compared (15,16). The database automatically generated box-and-whisker plots and provided P-values for significance based on Kruskal-Wallis test. The differences in the expression of target miRNAs in subgroups were further analyzed based on clinical stages and lymph node metastasis status (N0/N1/N2). When generating expression maps for multi-group comparisons, the statistical engine of the UALCAN platform automatically performs one-way analysis of variance (ANOVA) to assess overall differences in gene expression levels between groups. When ANOVA results indicate significant differences ($P<0.05$), the platform further employs Tukey's Honestly Significant Difference (HSD) post hoc test for pairwise comparisons to control for error rates arising from multiple comparisons. UALCAN was used to evaluate the relationship between target miRNA expression levels and overall survival in patients with COAD based on the Kaplan-Meier method (15). Patients were divided into high-expression and low-expression groups based on median expression values, and the log-rank test was used to compare survival curves between the two groups. All analytical results were exported directly from the platform and underwent partial formatting integration and annotation in GraphPad Prism.

Using the miRBase database via NCBI, the mature sequences of three miRNAs were retrieved and their corresponding ID numbers and standard nomenclature were collected (17,18). The miRNA IDs or standard nomenclature obtained was used, performing a search in the miRDB database and compiling the predicted target genes into an XLSX worksheet (17) for convenient further analysis of the associations among the three microRNAs. Target gene data were read and organized using the readxl package 1.4.5 (https://cran.r-project.org/package=readxl). Missing values were filtered for each column of miRNA target genes using the na.omit() function to construct the target gene set (19). The Reduce() and intersect() functions were used to calculate the common target points of the target gene sets, and output the number of genes in the intersection along with their specific list. Finally, the plotrix package 3.8.4 (https://cran.r-project.org/package=plotrix) was used to generate the Venn diagram. The target gene data was imported using the readxl package and the acquired data was processed and aggregated using the dplyr package 1.1.4 (https://cran.r-project.org/package=dplyr). The na.omit() function was applied to clean missing values in each target gene column (18). The cleaned data was created into a list object as the foundational data structure for subsequent UpSet plot analysis. The list was organized with corresponding miRNA names as keys and their target gene vectors as values to facilitate set operations and visualization mapping (20). The upset() function from the UpSetR package 1.4.0 (https://cran.r-project.org/package=UpSetR)was used to create an UpSet plot, converting data into the appropriate format via fromList(). Sets were sorted in descending order by intersection frequency (order.by='freq'), preserving the original set order (keep.order=TRUE), with set sizes indicated in steel blue (sets.bar.color='steelblue'). Finally, the axis labels to 'Intersection Size' (Y-axis of the main bar plot) and 'Set Size' (X-axis of the set size bar plot) were explicitly set to generate the UpSet plot.

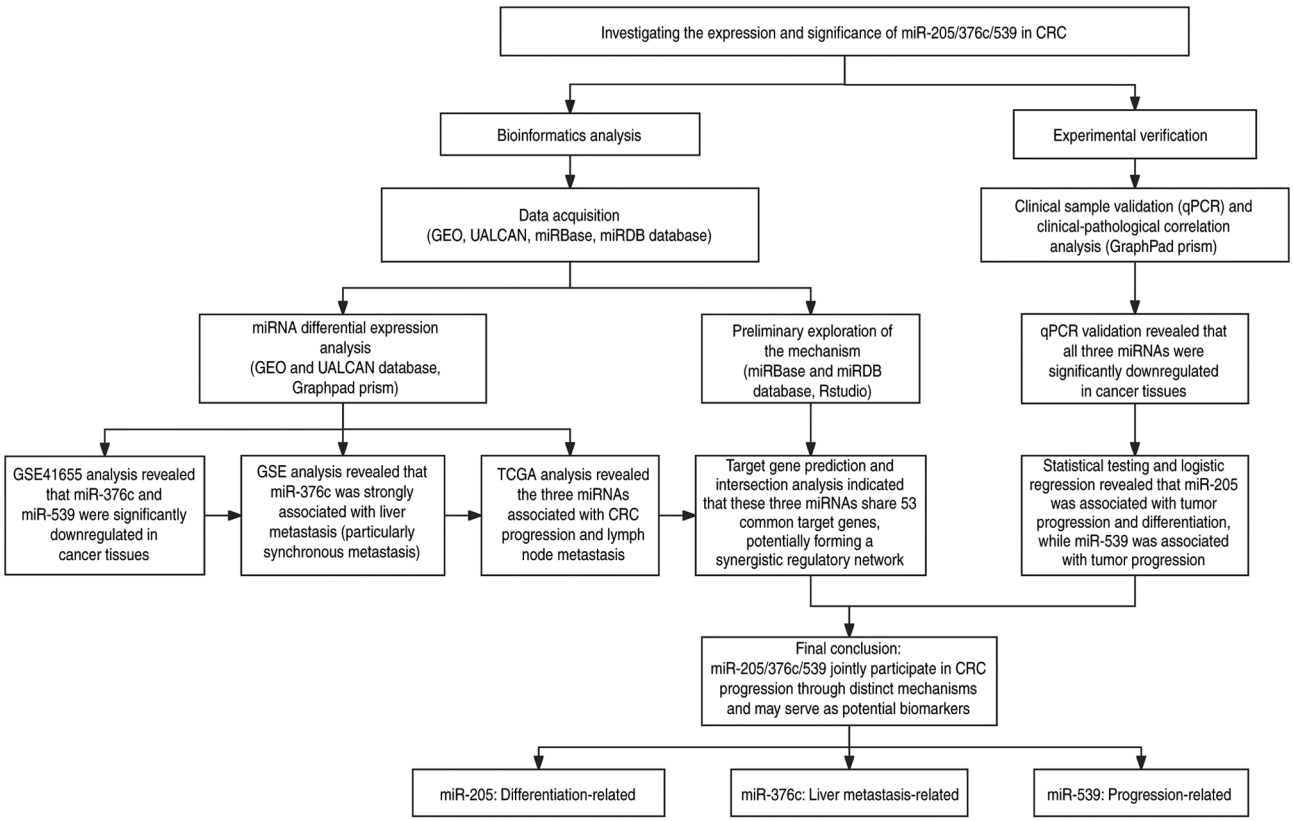

Figure 1. Overview of the study design and analytical workflow. The study employed a research framework of 'computer simulation analysis-experimental validation-integrated interpretation' to systematically investigate the expression patterns, clinical significance, and potential mechanisms of miR-205, miR-376c, and miR-539 in CRC. The flowchart clearly illustrates the entire process including: Obtaining data from public databases (GEO, UALCAN, miRBase, miRDB) for bioinformatics mining, collecting 25 clinical sample pairs for qPCR validation, and finally integrating analyses using statistical and bioinformatics tools. Key findings include: All three miRNAs were significantly downregulated in cancer tissues; miR-376c was associated with liver metastasis (particularly synchronous metastasis); miR-205 and miR-539 were associated with tumor differentiation, staging, and lymph node metastasis, respectively; target gene prediction revealed 53 common potential targets shared among the three miRNAs, suggesting their potential involvement in CRC progression through a synergistic regulatory network. This integrated flowchart visually represents the overall study approach from hypothesis validation to mechanistic exploration and highlights its main conclusions. CRC, colorectal cancer; miRNA or miR, microRNA.

Patients and tissue samples. Surgically resected CRC tissues were obtained from 25 patients at the Department of Gastrointestinal Surgery, Zhongshan Hospital, Xiamen University (Xiamen, China). Patient recruitment took place from January 2022 to October 2022, with all tissue samples collected in October 2022. The sample age ranged from 53 to 87 years old, with a median age of 66 years. The sample included 18 males and 7 females. All patient samples were obtained with written informed consent and approved [approval no. xmzsyyky (2024-703)] by the Ethics Committee of Zhongshan Hospital, Xiamen University (Xiamen, China). A total of 25 pairs of tissue specimens were collected, all from the initial surgical operations, without preoperative chemotherapy or radiotherapy. Each specimen was collected from CRC tissue and distal colorectal mucosa. Tissue samples were immediately frozen at -196˚C and subsequently stored in a refrigerator at -80˚C. The reverse transcription reaction mixture, consisting of total RNA templates extracted from the aforementioned colorectal cancer tissue and distal colorectal mucosa, reverse transcriptase (RT) enzyme, deoxyribonucleotide triphosphates (dNTPs), and RT reaction buffer, all of which were individually procured components included in the PrimeScript™ RT Reagent Kit (cat. no. RR037A, Takara Bio, Inc.), was gently mixed and incubated at 37˚C for 1 h to complete the reverse transcription reaction.

Reverse transcription-quantitative PCR (RT-qPCR). Total RNA was extracted from fresh frozen tissue samples using TRIzol reagent (Invitrogen; Thermo Fisher Scientific, Inc.) according to the manufacturer's instructions. RNA concentration and purity were assessed using a NanoDrop 2000 spectrophotometer (Thermo Fisher Scientific, Inc.), with the A260/A280 ratio maintained between 1.8 and 2.0. RNA integrity was verified by 1.5% agarose gel electrophoresis. A total of 1 μg of total RNA was used as a template and reverse transcription was performed using the TransScript® Green miRNA Two-Step qRT-PCR Super Mix kit (TransGen Biotech Co., Ltd.) to synthesize cDNA, according to the manufacturer's instructions.

qPCR reactions were performed using the Applied Biosystems QuantStudio 5 Real-Time Fluorescent Quantitative PCR System (Thermo Fisher Scientific, Inc.). The reaction system consisted of 20 μl in total, including 10 μl TransStart® Tip Green qPCR SuperMix (TransGen Biotech Co., Ltd.), 0.4 μl forward primer, 0.4 μl universal reverse primer, 2 μl cDNA template, and 7.2 μl nuclease-free water. The thermocycling conditions were as follows: Pre-denaturation

at 95˚C for 30 sec, followed by 40 cycles of denaturation at 95˚C for 5 sec and annealing/extension at 60˚C for 30 sec. Each sample was processed in triplicate, with a no-template control (NTC) included to rule out contamination. U6 snRNA was used as the reference gene, and the relative expression levels of miRNAs were calculated using the $2^{-\Delta\Delta Cq}$ method as previously described (21).

Data summary and statistical analysis. All statistical analyses were performed using Graphpad Prism 10.6.1 statistical software (Dotmatics). In the GSE41655 dataset, a normality test on the data was first performed. Subsequently, nonparametric Kruskal-Wallis test was used to analyze the results. If the test results were significant, Dunn's post hoc test was further performed for pairwise multiple comparisons. Based on the GSE81581 dataset and qPCR data results, paired t-test analysis was performed on the mean values of each group. Moreover, the results were combined with clinical data for comprehensive analysis according to sex, age, location, tumor stage, depth of invasion, and lymph node metastasis in patients with CRC and analyzed using Fisher's exact test. Univariate logistic regression was used to analyze miR-205 and miR-539 as potential risk factors associated with tumor progression. Two-tailed P<0.05 was considered to indicate a statistically significant difference. Spearman's ρ and Pearson's r correlation analyses were performed separately on the GSE41655 dataset and clinical sample qPCR data, with Bonferroni correction applied to the results.

Results

Differential expression and correlation of miR-205, miR-376c, and miR-539 between cancer and adjacent tissues in the GSE41655 dataset. To investigate the roles of the three miRNAs, miR-205, miR376c and miR-539, in CRC and normal colorectal tissues, their involvement in CRC pathogenesis was first analyzed using publicly available data from the GEO database. Based on the GSE41655 dataset, the Kruskal-Wallis test was employed to demonstrate significant differences among the three miRNA groups. Subsequently, using 15 normal colon tissue samples as controls, pairwise multiple comparisons were performed among the three miRNA groups via Dunn's test. It was found that miR-205 (P<0.05; Fig. 2A) and miR-376c (P<0.05; Fig. 2B) were downregulated in CRC tumor tissues compared with normal colon tissue. Furthermore, compared with normal colonic tissue, miR-539 expression was reduced in CRC tumor tissue (P<0.05; Fig. 2C), while no significant changes were observed in adenocarcinoma tissue (P<0.05; Fig. 2C). To further investigate the expression correlations among these three miRNAs in CRC, correlation heatmap analysis was performed using Pearson's r correlation analysis (Fig. 2D).The results indicated that there was no significant correlation in the expression of these three miRNAs in CRC (Fig. 2D).

miR-205, miR-376c, and miR-539 expression in tumor and normal tissues from clinical CRC specimens. To increase the credibility of the results, the expression levels of miR-205-5p, miR-376c-3p, and miR-539-5p were further detected among 25 patients with CRC by RT-qPCR. The expression levels of the miRNAs in cancer tissues were significantly decreased compared with corresponding adjacent healthy tissues: miR-205 (P<0.05; Fig. 3A), miR-376c (P<0.01; Fig. 3B) and miR-539 (P<0.05; Fig. 3C). To further investigate the correlation between the expression levels of the three miRNAs and their expression in CRC tumor tissues and adjacent normal tissues, correlation analysis was also performed using Pearson's r correlation analysis. The results revealed that miR-205 and miR-539 exhibited a strong correlation in their expression levels within cancerous tissues (Fig. 3D).

miR-376c is closely related to liver metastases, especially in the case of synchronous liver metastasis. In order to further explore the role of the aforementioned three microRNAs in the development of CRC, the GSE81581 dataset was used. Compared with primary CRC tissues, miRNA-376c expression was increased in CRC liver metastases (P<0.05; Fig. 4B), especially in the case of synchronous liver metastasis (Fig. 4E), while the expression levels of miR-205 (P>0.05; Fig. 4A) and miR-539 (P>0.05; Fig. 4C) were not significantly altered in CRC liver metastases. In addition, miR-376c expression exhibited no significant changes in CRC metachronous liver metastasis (P>0.05; Fig. 4C).

miR-205, miR-376c, and miR-539 are associated with CRC progression and prognosis. CRC is characterized by frequent metastasis, high invasiveness, and rapid development and high mortality. The expression of miR-205, miR-376c, and miR-539 was analyzed in the TCGA database via UALCAN. As revealed Fig. 5A-C, miR-376 expression was upregulated in primary cancer, while the expression levels of miR-205 and miR-539 were relatively high in normal tissues. The expression of miR-205, miR-376c, and miR-539 was closely associated with individual cancer stage (Fig. 5D-F) and lymph node metastasis (Fig. 4G-I), but showed no direct association with late survival (P>0.05; Fig. 5J-L).

Correlation analysis of miR-205, miR-376c, and miR-539 target genes. To further investigate the relationships among miR-205, miR-376c, and miR-539, the 5' and 3' mature sequences of these three miRNAs were obtained from the miRBase database. No significant common sequences identified among the mature forms of these three miRNAs (Fig. 6A). Subsequently, the predicted target genes of miR-205, miR-376c, and miR-539 were retrieved from the miRDB database and the relationships among these target genes were analyzed. Venn diagram analysis indicated that there were no common target genes among the six distinct sequences, miR-205-3p, miR-205-5p, miR-376c-3p, miR-376c-5p, miR-539-3p, and miR-539-5p (Fig. 6B). However, the UpSet plot revealed that the mature sequences of miR-205, miR-376c, and miR-539 (5p or 3p end sequences) share a total of 53 predicted target genes (Fig. 6C).

Distribution of miR-205, miR-376c, and miR-539 in patients with CRC and clinicopathological characteristics. To investigate the association of the miRNAs with clinicopathological characteristics, non-parametric tests were performed to analyze the relationships between miRNA expression and clinicopathological features in CRC samples. Based on the

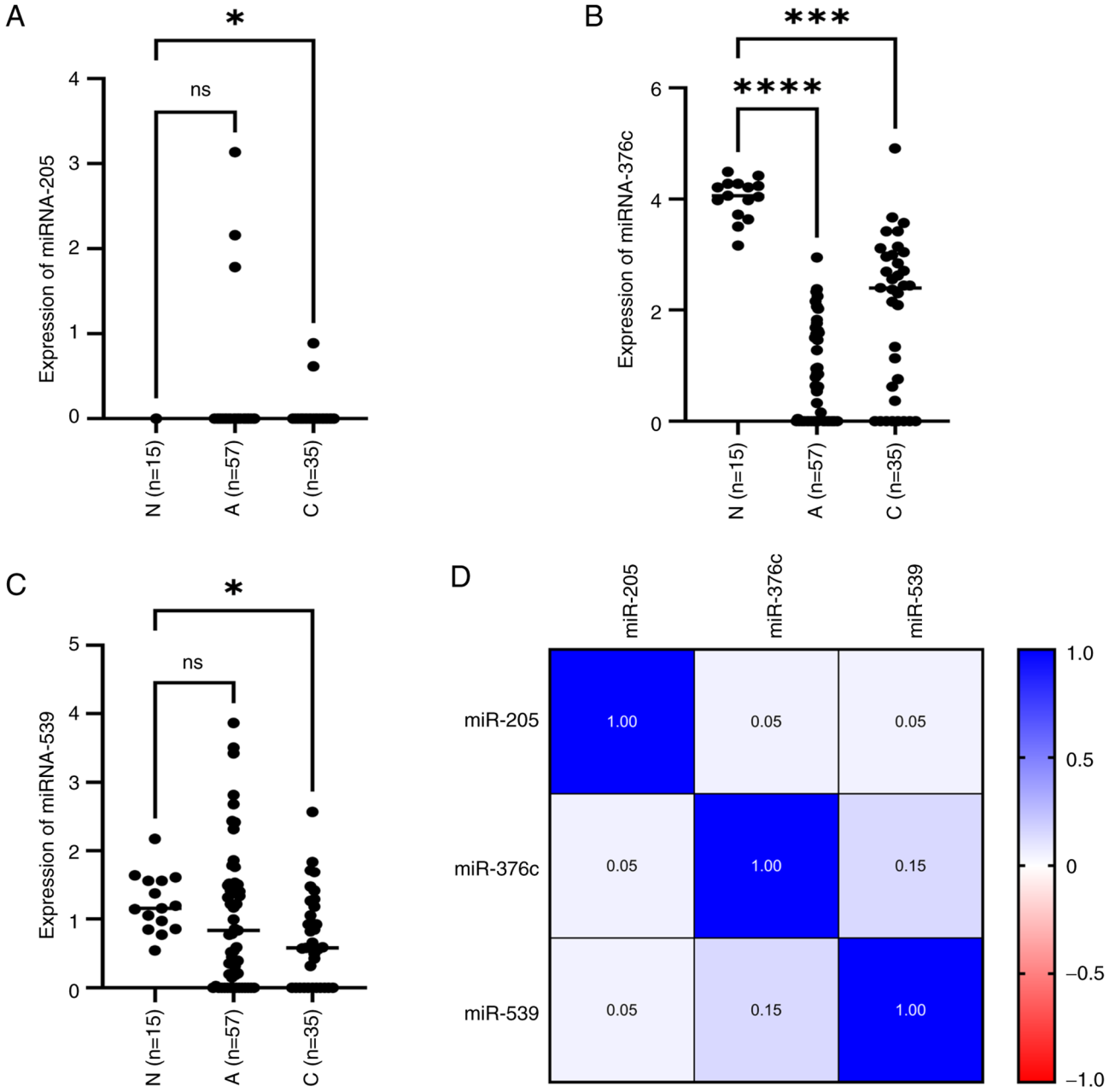

Figure 2. Expression profiles and correlation analysis of miR-205, miR-376c, and miR-539 in colorectal cancer and non-cancerous tissues from the GSE41655 dataset. The expression levels and correlation of miR-205, miR-376c and miR-539 in normal tissues and colorectal cancer tissues were analyzed in the GSE41655 dataset, which contained 35 colorectal tumor tissues, 15 matched adjacent tissues, and 57 colorectal adenoma tissues. (A) miR-205 expression. (B) miR-376c expression. (C) miR-539 expression. (D) Correlation analysis of the expression of miR-205, miR-376 and miR-539 in cancer tissues. N, normal tissues; A, adenoma tissues; C, colorectal cancer tumor tissues. *P<0.05, ***P<0.001 and ****P<0.0001. miR, microRNA; ns, not statistically significant.

experimental data obtained, the median expression levels of miR-205, miR-376c, and miR-539 in cancer tissues were calculated, and grouped by age (<60 years old, ≥60 years old), sex, tumor stage (stages I and II vs. III and IV), presence or absence of lymph node metastasis, tumor location (left or right colon), and degree of differentiation (low, moderate, or high). As shown in Tables I and III, miR-205 and miR-539 significantly differed according to tumor stage (P=0.0154) and lymph node metastasis (P=0.0154) in cancer tissues respectively, while no statistically significant differences were observed for the other clinicopathological factors. No significant associations were observed between the expression of miR-376c and any of the six clinicopathological characteristics (Table II). In addition, logistic regression analysis indicated that miR-205 may be a potential risk factor associated with tumor progression and differentiation, while miR-539 may be a potential risk factor associated with tumor progression (Table IV).

Discussion

The current prognosis for CRC is still not optimistic, and its tumor progression is a multi-step process involving changes at the genetic and epigenetic levels (1,2). miRNAs are widely distributed in numerous eukaryotes, and the transcription of miRNA genes is synchronized with other genes (22). Notably, >60% of human protein-coding genes are predicted to contain

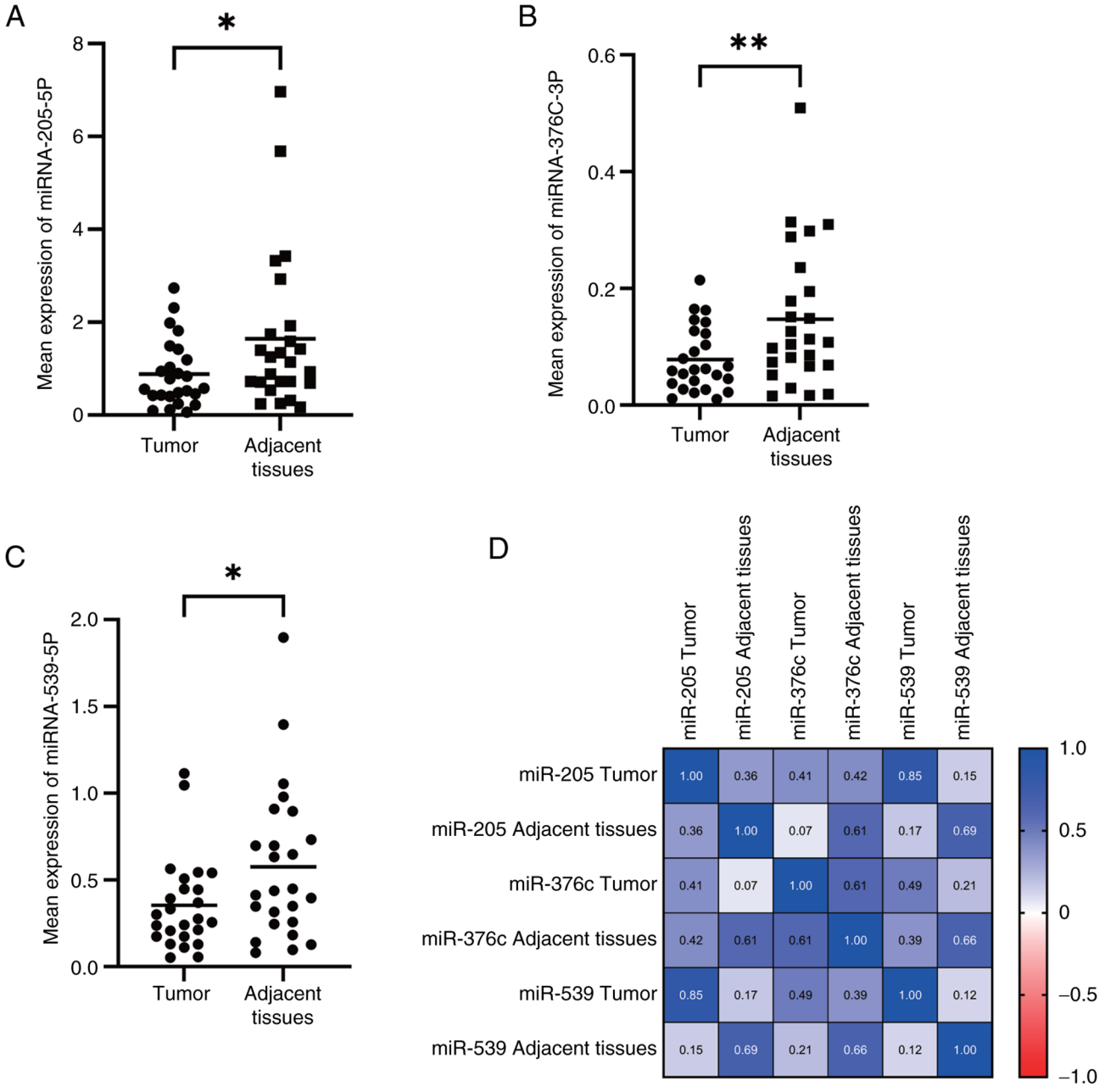

Figure 3. Expression levels of miR-205, miR-376c and miR-539 are significantly different between CRC tissues and adjacent tissues, as assessed using RT-qPCR. (A) Comparison of miR-205 expression levels in human CRC tissues and matched adjacent tissues. (B) Comparison of miR-376c expression levels in human CRC tissues and matched adjacent tissues. (C) Comparison of miR-539 expression levels in human CRC tissues and matched adjacent tissues. miRNA expression was quantified by RT-qPCR and normalized to that in the matched adjacent normal tissues. (D) Correlation analysis of the expression of miR-205, miR-376 and miR-539 in tumor and normal tissues. *P<0.05 and **P<0.01. miR, microRNA; CRC, colorectal cancer; RT-qPCR, reverse transcription quatitative PCR.

conserved targets of miRNA, mainly in the 3' UTR. Therefore, miRNAs play important regulatory roles in cell differentiation, proliferation, apoptosis, and other pathological processes (23). miRNAs can function as oncogenes or tumor suppressor genes based on their corresponding regulated mRNA sequences. miRNAs exert regulatory functions by binding to mRNA targets, disrupting mRNA stability or inhibiting translation (2-4). There are numerous studies on miRNAs in various cancers (3,4). However, it is unclear whether various miRNAs play different roles in CRC.

miRNAs also play important roles in tumor biology, including tumor evolution, invasion, metastasis, and angiogenesis (24). In the present study, the differences in the expression levels of miR-205, miR-376c, and miR-539 between CRC and adjacent tissues in 25 CRC patients were analyzed and found significant differences in the expression levels of the three miRNAs in cancer and matched normal tissues.

According to previous studies, miR-205 expression is significantly reduced in glioma (25), head and neck squamous cell carcinoma (26), thyroid cancer (27), prostate cancer (28), renal cell carcinoma (29), pancreatic cancer (30) and hepatocellular carcinoma (31). miR-205 has also been reported to contribute to distinguishing between high-grade and low-grade endometrioid tumors (32). High expression of mature miR-205

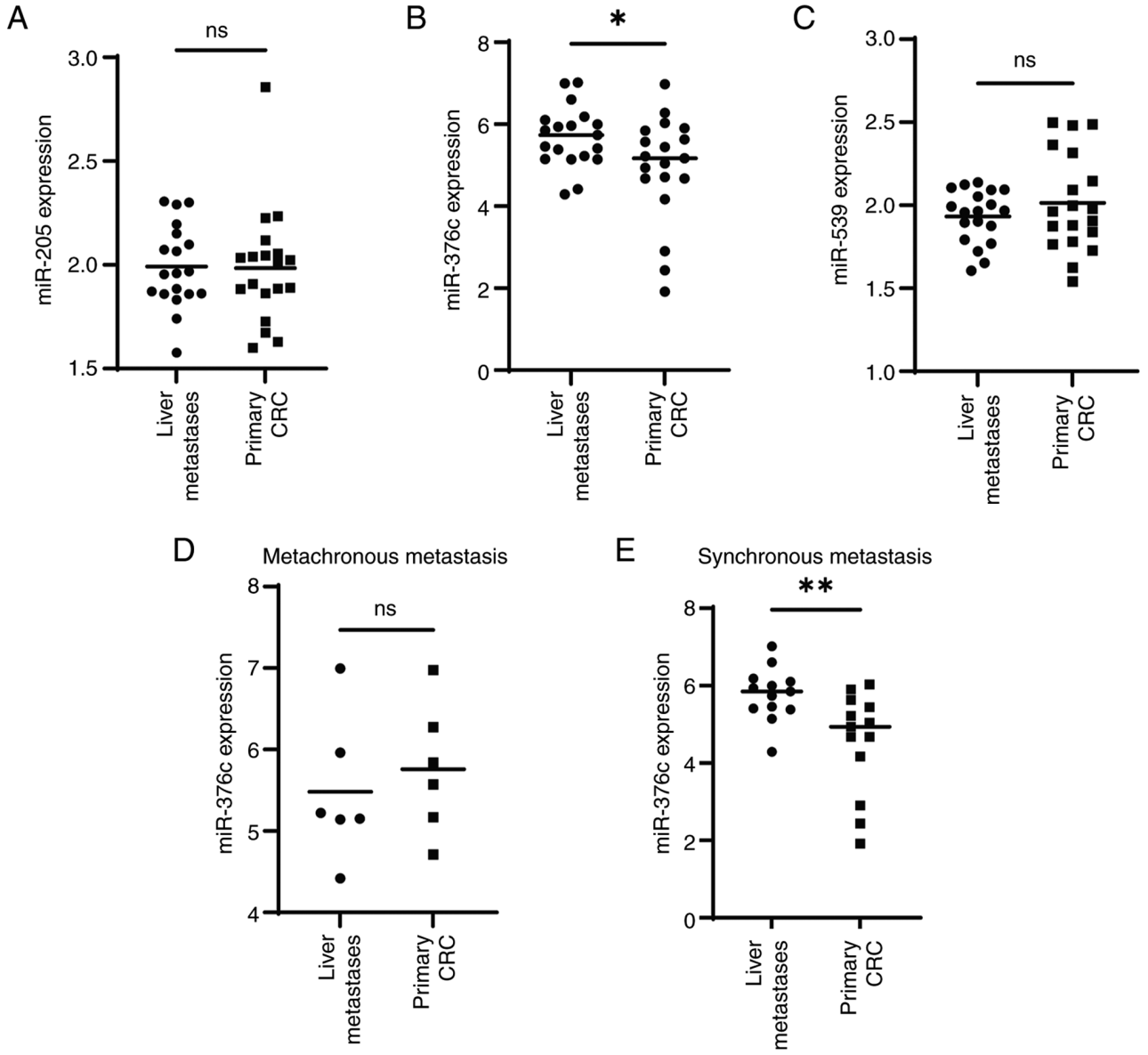

Figure 4. Relationship between the relative expression levels of miR-205, miR-376c and miR-539, and the presence or absence of liver metastasis in the GSE81581 dataset. (A) Relationship between miR-205 expression and CRC liver metastasis. (B) Relationship between miR-376c expression and CRC liver metastasis. (C) Relationship between miR-539 expression and CRC liver metastasis. (D) Relationship between miR-376c expression and metachronous liver metastasis. (E) Relationship between miR-376c expression and synchronous liver metastasis. *P<0.05 and **P<0.01. miR, microRNA; CRC, colorectal cancer; ns, not statistically significant.

was revealed to be associated with lymph node-positive status in patients with esophageal squamous cell carcinoma (33), and experiments have shown that upregulation of miR-205 *in vitro* reduces cell viability, migration, and invasion in gliomas. In the clinical tissues of the present study, RT-qPCR showed that the expression levels of miR-205 in CRC tissues were significantly downregulated compared with adjacent tissues (P<0.05). These results are consistent with previous studies and demonstrate that miR-205 could act as a potential therapeutic target for CRC (25-33).

As a large miRNA cluster, members of the miR-376 family have been found to be susceptible to changes in various human cancers. For instance, POU2F2-mediated upregulation of lncRNA PTPRG-AS1 inhibited ferroptosis in breast cancer via the miR-376c-3p/SLC7A11 axis (34), and MEG3 suppressed angiogenesis through the miR-376a/RASA1 axis in ovarian carcinoma-derived microvascular endothelial cells (35). miR-376a expression was lower in glioma cells than in normal astrocytes. miR-376a mimic inhibited SIRT1, YAP1, and VEGF expression and suppressed the proliferation, migration and angiogenesis abilities of the glioma cell lines LN229 and A172, whereas miR-376a inhibitor exerted the opposite effects (36). Since substantial progress has been recorded in research on miR-376a and miR-376b, miR-376c was selected as a research target (35-37). The present study showed that miR-376c was downregulated in CRC tissues, with significant differences in expression between tumor and adjacent tissues, indicating that miR-376c may be involved in the development of CRC. Further bioinformatics analyses suggested that it is potentially associated with CRC liver metastasis.

Furthermore, the expression of miR-539 in CRC was evaluated. It is well-known that aberrant expression of

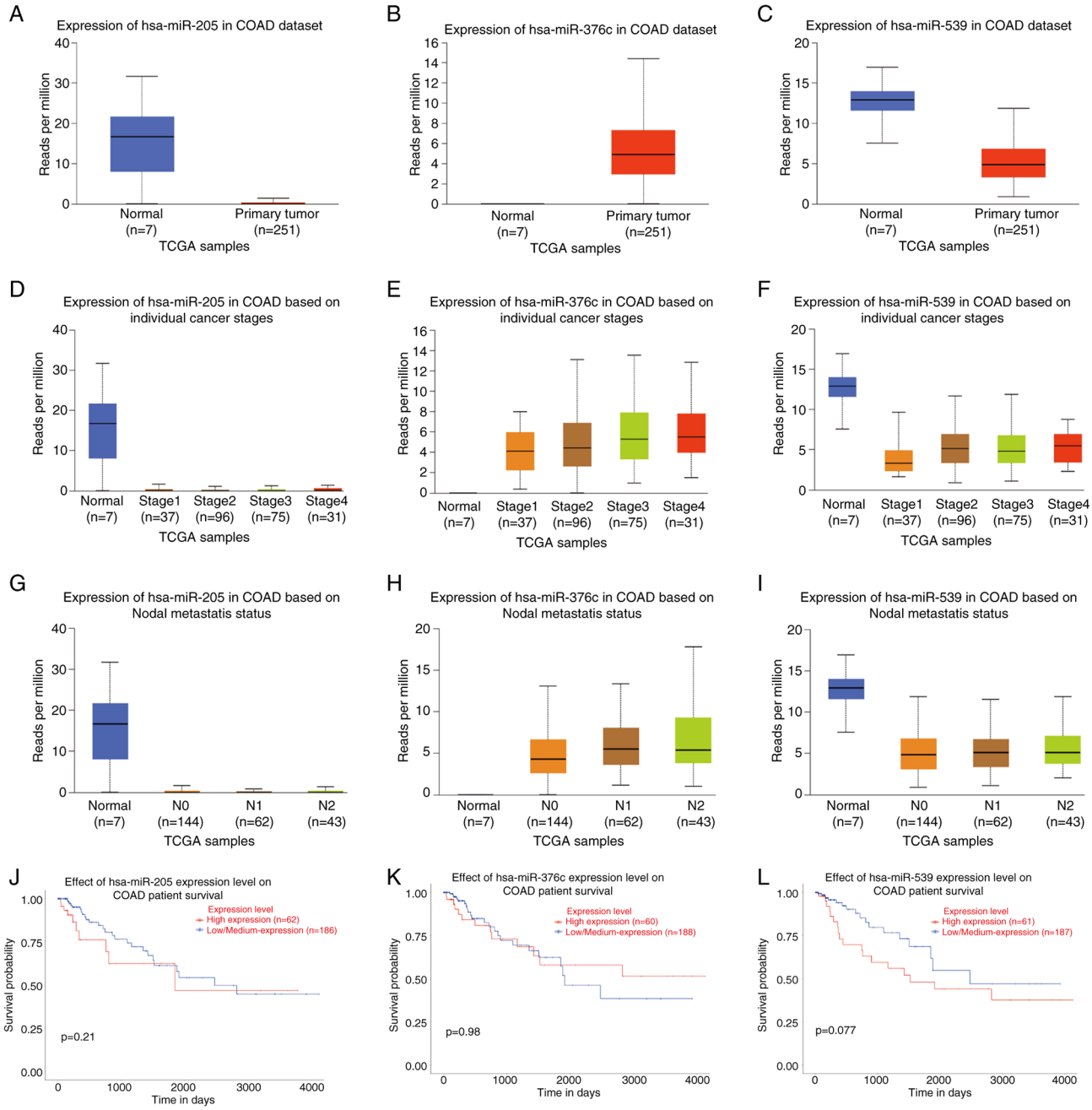

Figure 5. Relationship between the relative expression levels of miR-205, miR-376c and miR-539, and the development of CRC. (A-C) The expression of miR-205, miR-376c and miR-539 in healthy individuals and patients with CRC was analyzed using UALCAN. (D-F) The expression of miR-205, miR-376c and miR-539 in COAD based on individual cancer stages was analyzed using UALCAN. (G-I) The expression of miR-205, miR-376c and miR-539 in COAD based on nodal metastatis status was analyzed using UALCAN. (J-L) The effects of miR-205, miR-376c and miR-539 expression levels on the survival of patients with COAD was analyzed using UALCAN. miR, microRNA; CRC, colorectal cancer; COAD, colorectal adenocarcinoma.

miR-539 plays an important role in the initiation and development of several cancers. For instance, miR-539 was revealed to act as a tumor suppressor in hepatocellular carcinoma (HCC) (38), thyroid cancer (39), breast cancer (40), and osteosarcoma (41). Furthermore, miR-539 was shown to be upregulated in hepatocellular carcinoma and may be involved in regulating autophagy gene expression (42). Consistent with the aforementioned previous research, the present study showed that miR-539 is downregulated in CRC tissues, with significant differences in its expression according to tumor stage and lymph node metastasis. In a previous study, miR-539 was demonstrated to promote ferroptosis in CRC by directly targeting TIPE to activate the SAPK/JNK signaling pathway (43). Zhao *et al* (44) reported that miR-539 was downregulated in CRC tissues and cell lines, but was negatively associated with advanced clinical stage and lymph node metastasis. Therefore, further research is needed to clarify its role.

In the present study, significant differences were found in the expression of the three miRNAs between tumor tissues and corresponding normal tissues in the GEO database. In the GSE41655 dataset, the overall expression trends of miR-376c, miR-539, and miR-205 between tumor and normal tissues were consistent with the results from our 25 clinical samples. In

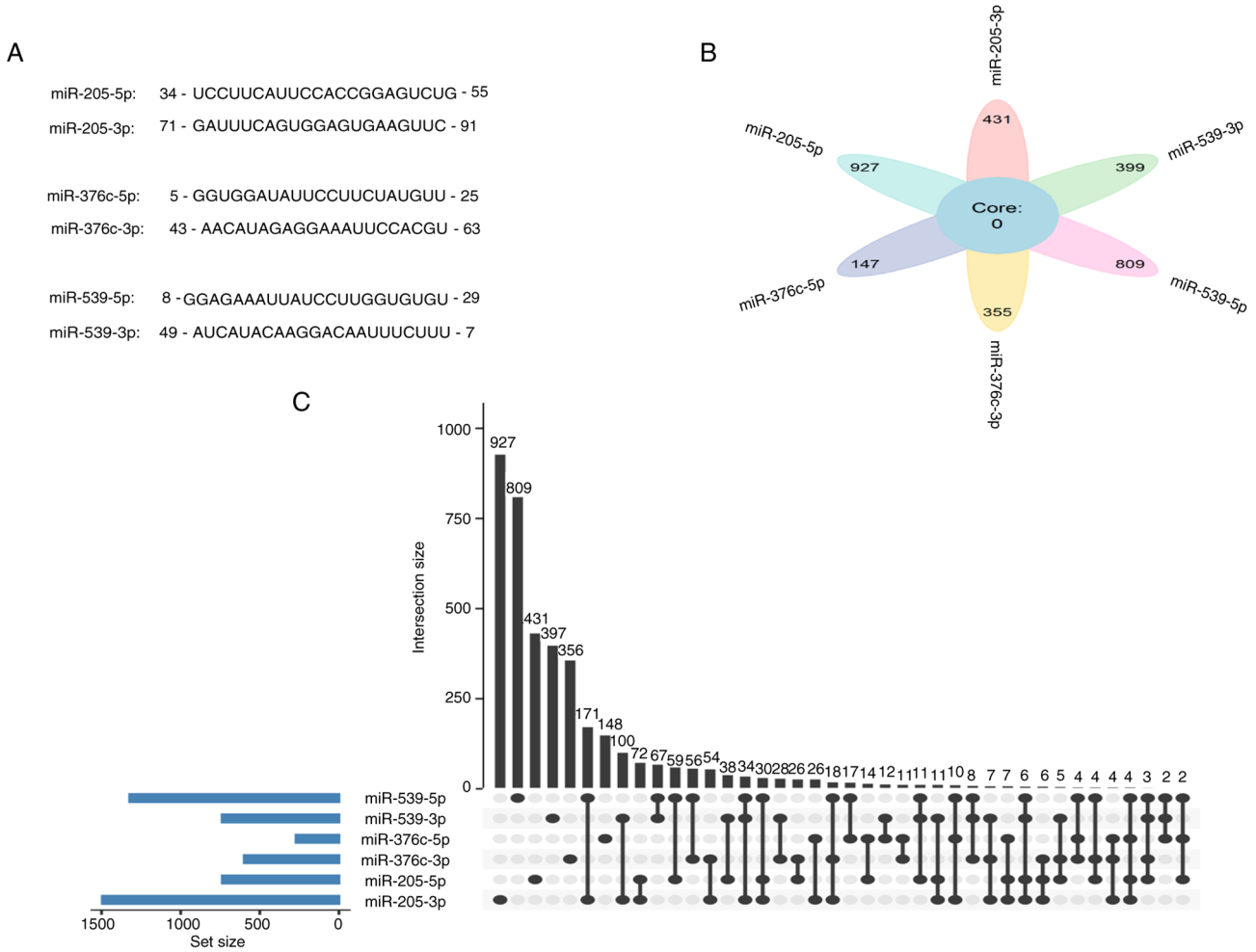

Figure 6. Sequences of miR-205, miR-376, and miR-539 collected from the miRBase database, and predicted target genes for miR-205, miR-376, and miR-539 mined from the miRDB database for correlation analysis. (A) 5p and 3p mature sequences of miR-205, miR-376c, and miR-539. (B) UpSet plot of the target gene intersection analysis for the 5p and 3p mature sequences of miR-205, miR-376, and miR-539. (C) Venn diagram of the target gene intersection analysis for the 5p and 3p mature sequences of miR-205, miR-376, and miR-539. miR, microRNA.

addition, in the GSE81581 dataset, only the expression trend of miR-376c was correlated with CRC liver metastasis. To investigate whether the three miRNAs interact with one another during the development of CRC, the expression levels of miR-205, miR-376c, and miR-539 were analyzed and varying degrees of positive correlation was found. Moreover, the ratios of expression levels in cancer tissues to adjacent tissues also showed a certain degree of positive correlation. These findings revealed the simultaneous expression pattern of the three miRNAs in CRC, and suggest that miR-205, miR-376c, and miR-539 may play different roles in the occurrence and development of CRC. While the relevant molecular mechanisms remain unclear, their target genes should be validated in future studies.

Additionally, the mature sequences of the three miRNAs were collected from the miRBase database and found no significant common sequences among them. To further investigate the relationships among their mechanisms of action, bioinformatics analysis was employed to reveal potential associations between miR-205, miR-376c, and miR-539 at the target gene level. The Venn diagram analysis indicated that no common target genes were shared among the six distinct sequences, miR-205-3p, miR-205-5p, miR-376c-3p, miR-376c-5p, miR-539-3p, and miR-539-5p. However, the UpSet plot revealed that the mature sequences of miR-205, miR-376c, and miR-539 (5p or 3p end sequences) share a total of 53 predicted target genes. This finding suggests that despite differences in their expression patterns and functions, these three factors may exert synergistic effects in the development of CRC by regulating partially overlapping downstream gene networks. These common target genes may be involved in classical tumor-related pathways such as Wnt/β-catenin and PI3K/AKT (45,46), but their specific functions and regulatory mechanisms require further experimental investigation and validation.

miR-205 and miR-539 upregulation predicted advanced TNM stage and poor tumor differentiation according logistic regression analysis. However, they were downregulated in tumor tissues compared with normal tissues. It is speculated that they may be downregulated in early tumor development, and become upregulated during tumor progression, thus exhibiting different roles at different stages of CRC. Given that numerous miRNAs are altered in CRC, these three miRNAs were randomly selected based on previous studies (43-46), as they exhibited significant correlations with clinicopathological characteristics. Future

Table I. Distribution of miR-205 expression relative to normal adjacent tissue and clinicopathological characteristics in patients with colorectal cancer.

Characteristics	No. of patients	Downregulated (%)	Upregulated (%)	P-value
Age (years)				>0.9999
<60	6	3 (12)	3 (12)	
≥60	19	11 (44)	8 (32)	
Sex				0.6564
Female	7	3 (12)	4 (16)	
Male	18	11 (44)	7 (28)	
TNM stage				0.0154[a]
I, II	12	10 (40)	2 (8)	
III, IV	13	4 (16)	9 (36)	
Lymphatic metastasis				0.0154[a]
N=0	12	10 (40)	2 (8)	
N≠0	13	4 (16)	9 (36)	
Location				>0.9999
Left	17	9 (36)	8 (32)	
Right	8	5 (20)	3 (12)	
Differentiation				0.3500
Low	6	2 (8)	4 (16)	
Middle	19	12 (48)	7 (28)	

[a]P<0.05. miR, microRNA.

Table II. Distribution of miR-376c expression relative to normal adjacent tissue and clinicopathological characteristics in patients with colorectal cancer.

Characteristics	No. of patients	Downregulated (%)	Upregulated (%)	P-value
Age (years)				0.5623
<60	6	4 (16)	2 (8)	
≥60	19	16 (64)	3 (12)	
Sex				0.1130
Female	7	4 (16)	3 (12)	
Male	18	16 (64)	2 (8)	
TNM stage				0.1602
I, II	12	8 (32)	4 (16)	
III, IV	13	12 (48)	1 (4)	
Lymphatic metastasis				0.1602
N=0	12	8 (32)	4 (16)	
N≠0	13	12 (48)	1 (4)	
Location				>0.9999
Left	17	13 (52)	4 (16)	
Right	8	7 (28)	1 (4)	
Differentiation				>0.9999
Low	6	5 (20)	1 (4)	
Middle	19	15 (60)	4 (16)	

miR, microRNA.

studies should included larger sample sizes and additional miRNAs.

The primary strength of this study lies in its cross-referencing of multiple databases, integrating bioinformatics

Table III. Distribution of miR-539 expression relative to normal adjacent tissue and clinicopathological characteristics in patients with colorectal cancer.

Characteristics	No of patients	Downregulated (%)	Upregulated (%)	P-value
Age (years)				>0.9999
<60	6	3 (12)	3 (12)	
≥60	19	11 (44)	8 (32)	
Sex				0.6564
Female	7	3 (12)	4 (16)	
Male	18	11 (44)	7 (28)	
TNM stage				0.0154[a]
I, II	12	10 (40)	2 (8)	
III, IV	13	4 (16)	9 (36)	
Lymphatic metastasis				0.0154[a]
N=0	12	10 (40%)	2 (8%)	
N≠0	13	4 (16%)	9 (36%)	
Location				>0.9999
Left	17	10 (40)	7 (28)	
Right	8	4 (16)	4 (16)	
Differentiation				0.3500
Low	6	2 (8)	4 (16)	
Middle	19	12 (48)	7 (28)	

[a]P<0.05. miR, microRNA.

Table IV. Logistic regression analysis between miR-205, miR-539 and pathological characteristics.

	miR-205 (upregulated)			miR-539 (upregulated)		
Pathological characteristics	OR	95% CI	P-value	OR	95% CI	P-value
Advanced TNM stage (III, IV)	11.25	1.905-100.1	0.0136	11.25	1.905-100.1	0.0136[a]
N≥1	11.25	1.905-100.1	0.0136	11.25	1.905-100.1	0.0136[a]
Differentiation (poor)	10.83	1.362-233.3	0.0474	3.429	0.5273-29.75	0.2124

[a]P<0.05. miR, microRNA; OR, odds ratio; CI, confidence interval.

with experimental validation methods to systematically investigate the expression patterns, clinical significance, and target gene networks of miR-205, miR-376c, and miR-539 in CRC. Additionally, advanced visualization tools such as UpSet plots were employed to identify 53 predicted target genes common these three miRNAs, suggesting potential synergistic regulatory interactions among them. However, the present study has several limitations, including a small sample size that may affect statistical power, lack of experimental validation on the relevant functions and pathways of the predicted target genes, and insufficient functional mechanism studies. Future studies should expand the sample size, and further validate and explore the target genes and functional mechanisms of these miRNAs through *in vitro* and *in vivo* experiments. Additionally, future studies may explore the specific mechanisms underlying the role of miRNA methylation patterns in CRC survival and staging through investigation of miR-205, miR-376c, and miR-539 miRNA methylation levels.

In conclusion, growing evidence indicates that miRNA signatures are associated with diagnosis, prognosis, progression, metastasis, and drug resistance of CRC. The present study revealed the expression patterns of miR-205, miR-376c, and miR-539 in CRC and their relationships with clinical features, such as sex and age, and provided evidence of the role of these three miRNAs, and that co-expression of these miRNAs exerts a synergistic regulatory role in the pathogenesis of CRC. miR-205, miR-376c, and miR-539 may participate in the development and progression of CRC. miR-205 and miR-539 may act as potential risk factors predicting advanced pathological stage and tumor differentiation. Overall, the findings confirmed that miR-205, miR-376c, and miR-539 are aberrantly expressed in CRC and closely associated with clinical and pathological characteristics. Target gene intersection

analysis further suggests that these three miRNAs may synergistically regulate CRC progression by sharing common downstream targets. Therefore, targeting these miRNAs or their co-regulated pathways may provide novel therapeutic strategies for CRC. Future research should focus on validating the functions of these shared target genes and their specific mechanisms of action in CRC.

Acknowledgements

The authors would like to thank the Zhongshan Hospital of Xiamen University for providing clinical samples and the contributions and support of the entire research team.

Funding

The present study was supported by the Natural Science Foundation of Fujian Province (grant no. 2021J01013), Natural Science Foundation of Xiamen (grant no. 3502Z20227104) and the the Natural Science Foundation of Jiangxi Province, China (grant no. 20242BAB25511).

Availability of data and materials

The data generated in the present study may be requested from the corresponding author.

Authors' contributions

JZ, GZ, ZL and CY contributed to the conception of this study and performed the preliminary documentation. All authors participated in the design of the study and implemented the research. JZ, CY, ZL, HR, KQ, ZC, and AB examined the archives, identified the cases included in the study, and collected the pathological information. ZL, XC, and CW enrolled patients in the study, performed clinical diagnosis, and collected clinical data. LS is responsible for bioinformatics database analysis, manuscript revisions, and responses to the comments of the reviewers. All authors participated in the statistical analysis and contributed to the interpretation of the results as well as the writing of the study. JZ and ZL confirm the authenticity of all the raw data. All authors reviewed all data, as well as read and approved the final manuscript.

Ethics approval and consent to participate

The present study abides by international and national regulations in accordance with the Declaration of Helsinki, and was approved [approval no. xmzsyyky (2024-703)] by the Ethics Committee of Zhongshan Hospital, Xiamen University (Xiamen, China). All patients provided written informed consent before being included in the study.

Patient consent for publication

Not applicable.

Competing interests

The authors declare that they have no competing interests.

References

1. Morgan E, Arnold M, Gini A, Lorenzoni V, Cabasag CJ, Laversanne M, Vignat J, Ferlay J, Murphy N and Bray F: Global burden of colorectal cancer in 2020 and 2040: Incidence and mortality estimates from GLOBOCAN. Gut 72: 338-344, 2023.
2. Zhu L, Wang R, Zhang L, Zuo C, Zhang R and Zhao S: rs187960998 polymorphism in miR-211 prevents development of human colon cancer by deregulation of 3'UTR in CHD5. Onco Targets Ther 12: 405-412, 2019.
3. Li D, Wang Q, Li N and Zhang S: miR-205 targets YAP1 and inhibits proliferation and invasion in thyroid cancer cells. Mol Med Rep 18: 1674-1681, 2018.
4. Cui X, Zhang A, Liu J, Wu K, Chen Z and Wang Q: Down-regulation of MAP2K1 by miR-539 inhibits hepatocarcinoma progression. Biochem Biophys Res Commun 504: 784-791, 2018.
5. Truong AD, Rengaraj D, Hong Y, Hoang CT, Hong YH and Lillehoj HS: Differentially expressed JAK-STAT signaling pathway genes and target microRNAs in the spleen of necrotic enteritis-afflicted chicken lines. Res Vet Sci 115: 235-243, 2017.
6. Wu Y, Park J, Xu E, Kim D, Lee J and Oh YK: MicroRNA-induced reprogramming of tumor-associated macrophages for modulation of tumor immune microenvironment. J Control Release 381: 113593, 2025.
7. Xing Y, Ruan G, Ni H, Qin H, Chen S, Gu X, Shang J, Zhou Y, Tao X and Zheng L: Tumor immune microenvironment and its related miRNAs in tumor progression. Front Immunol 12: 624725, 2021.
8. Wen D, Li S, Jiang W, Zhu J, Liu J and Zhao S: Retraction notice to 'MiR-539 inhibits human colorectal cancer progression by targeting RUNX2' [Biomed. Pharmacother. 95 (2017) 1314-1320]. Biomed Pharmacother 167: 115375, 2023.
9. Du Y, Rokavec M and Hermeking H: Squalene epoxidase/SQLE is a candidate target for treatment of colorectal cancers with p53 mutation and elevated c-MYC expression. Int J Biol Sci 19: 4103-4122, 2023.
10. Wang Y, Wu Y, Cai A, Ma C, Cai S, Wang H, Que Y, Xu S, Xu T and Hu Y: Cisplatin inhibits the proliferation of Saos-2 osteosarcoma cells via the miR-376c/TGFA pathway. Bosn J Basic Med Sci 21: 163-173, 2021.
11. Zhang Z, Yang L, Yao X, Yang M and Li G: LncRNA-ZNF281 interacts with miR-539 to promote hepatocellular carcinoma cell invasion and migration. Cancer Biother Radiopharm 35: 137-142, 2020.
12. Sayagués JM, Corchete LA, Gutiérrez ML, Sarasquete ME, Del Mar Abad M, Bengoechea O, Fermiñán E, Anduaga MF, Del Carmen S, Iglesias M, *et al*: Genomic characterization of liver metastases from colorectal cancer patients. Oncotarget 7: 72908-72922, 2016.
13. Barrett T, Wilhite SE, Ledoux P, Evangelista C, Kim IF, Tomashevsky M, Marshall KA, Phillippy KH, Sherman PM, Holko M, *et al*: NCBI GEO: Archive for functional genomics data sets-update. Nucleic Acids Res 41 (Database Issue): D991-D995, 2013.
14. Gustavsson EK, Zhang D, Reynolds RH, Garcia-Ruiz S and Ryten M: ggtranscript: An R package for the visualization and interpretation of transcript isoforms using ggplot2. Bioinformatics 38: 3844-3846, 2022.
15. Chandrashekar DS, Bashel B, Balasubramanya SAH, Creighton CJ, Ponce-Rodriguez I, Chakravarthi BVSK and Varambally S: UALCAN: A portal for facilitating tumor subgroup gene expression and survival analyses. Neoplasia 19: 649-658, 2017.
16. Cancer Genome Atlas Network: Comprehensive molecular characterization of human colon and rectal cancer. Nature 487: 330-337, 2012.
17. Kozomara A, Birgaoanu M and Griffiths-Jones S: miRBase: From microRNA sequences to function. Nucleic Acids Res 47 (D1): D155-D162, 2019.
18. Ranjbar R, Behzadi P and Mammina C: Respiratory tularemia: Francisella tularensis and microarray probe designing. Open Microbiol J 10: 176-182, 2016.
19. Jia A, Xu L and Wang Y: Venn diagrams in bioinformatics. Brief Bioinform 22: bbab108, 2021.
20. Lex A, Gehlenborg N, Strobelt H, Vuillemot R and Pfister H: UpSet: Visualization of intersecting sets. IEEE Trans Vis Comput Graph 20: 1983-1992, 2014.
21. Livak KJ and Schmittgen TD: Analysis of relative gene expression data using real-time quantitative PCR and the 2(-Delta Delta C(T)) method. Methods 25: 402-408, 2001.

22. Bai H, Dai Y, Fan P, Zhou Y, Wang X, Chen J, Jiao Y, Du C, Huang Z, Xie Y, *et al*: The METHYLTRANSFERASE B-SERRATE interaction mediates the reciprocal regulation of microRNA biogenesis and RNA m^6A modification. J Integr Plant Biol 66: 2613-2631, 2024.
23. Bartel DP: Metazoan MicroRNAs. Cell 173: 20-51, 2018.
24. Engler DB, Leonardi I, Hartung ML, Kyburz A, Spath S, Becher B, Rogler G and Müller A: Helicobacter pylori-specific protection against inflammatory bowel disease requires the NLRP3 inflammasome and IL-18. Inflamm Bowel Dis 21: 854-861, 2015.
25. De Bacco F, Orzan F, Erriquez J, Casanova E, Barault L, Albano R, D'Ambrosio A, Bigatto V, Reato G, Patanè M, *et al*: ERBB3 overexpression due to miR-205 inactivation confers sensitivity to FGF, metabolic activation, and liability to ERBB3 targeting in glioblastoma. Cell Rep 36: 109455, 2021.
26. Emmett SE, Stark MS, Pandeya N, Panizza B, Whiteman DC and Antonsson A: MicroRNA expression is associated with human papillomavirus status and prognosis in mucosal head and neck squamous cell carcinomas. Oral Oncol 113: 105136, 2021.
27. Li HN, Zhang HM, Li XR, Wang J, Xu T, Li SY, Dong ML, Wang G, Cui XQ, Yang X, *et al*: MiR-205-5p/GGCT attenuates growth and metastasis of papillary thyroid cancer by regulating CD44. Endocrinology 163: bqac022, 2022.
28. Kalogirou C, Linxweiler J, Schmucker P, Snaebjornsson MT, Schmitz W, Wach S, Krebs M, Hartmann E, Puhr M, Müller A, *et al*: MiR-205-driven downregulation of cholesterol biosynthesis through SQLE-inhibition identifies therapeutic vulnerability in aggressive prostate cancer. Nat Commun 12: 5066, 2021.
29. Huang W, Wu K, Wu R, Chen Z, Zhai W and Zheng J: Bioinformatic gene analysis for possible biomarkers and therapeutic targets of hypertension-related renal cell carcinoma. Transl Androl Urol 9: 2675-2687, 2020.
30. Zhu H, Shan Y, Ge K, Lu J, Kong W and Jia C: LncRNA CYTOR promotes pancreatic cancer cell proliferation and migration by sponging miR-205-5p. Pancreatology 20: 1139-1148, 2020.
31. Zhang H, Zhang G, Lu S, Zhang X and Yu J: Integrated analysis of ncRNA in hepatocellular carcinoma with CTNNB1 mutations reveals miR-205-5p and miR-3940-3p axes. Dig Liver Dis 57: 51-61, 2025.
32. Donkers H, Hirschfeld M, Weiß D, Erbes T, Jaeger M, Pijnenborg JMA, Bekkers R and Galaal K; ENITEC-consortium: Usefulness of microRNA detection in the diagnostics of endometrial cancer. Acta Obstet Gynecol Scand 100: 1148-1154, 2021.
33. Ibuki Y, Nishiyama Y, Tsutani Y, Emi M, Hamai Y, Okada M and Tahara H: Circulating microRNA/isomiRs as novel biomarkers of esophageal squamous cell carcinoma. PLoS One 15: e0231116, 2020.
34. Li J, Li PT, Wu W, Ding BN, Wen YG, Cai HL, Liu SX, Hong T, Zhang JF, Zhou JD, *et al*: POU2F2-mediated upregulation of lncRNA PTPRG-AS1 inhibits ferroptosis in breast cancer via miR-376c-3p/SLC7A11 axis. Epigenomics 16: 215-231, 2024.
35. Li Y, Zhang L, Zhao Y, Peng H, Zhang N and Bai W: MEG3 sponges miRNA-376a and YBX1 to regulate angiogenesis in ovarian cancer endothelial cells. Heliyon 9: e13204, 2023.
36. Deng YW, Shu YG and Sun SL: miR-376a inhibits glioma proliferation and angiogenesis by regulating YAP1/VEGF signalling via targeting of SIRT1. Transl Oncol 15: 101270, 2021.
37. Liu XW, Zhang CC and Zhang T: MiR-376b-3p functions as a tumor suppressor by targeting KLF15 in non-small cell lung cancer. Eur Rev Med Pharmacol Sci 24: 9480-9486, 2020.
38. Liu X, Chen D, Chen H, Wang W, Liu Y, Wang Y, Duan C, Ning Z, Guo X, Otkur W, *et al*: YB1 regulates miR-205/200b-ZEB1 axis by inhibiting microRNA maturation in hepatocellular carcinoma. Cancer Commun (Lond) 41: 576-595, 2021.
39. Gu L and Sun W: MiR-539 inhibits thyroid cancer cell migration and invasion by directly targeting CARMA1. Biochem Biophys Res Commun 464: 1128-1133, 2015.
40. Guo J, Gong G and Zhang B: miR-539 acts as a tumor suppressor by targeting epidermal growth factor receptor in breast cancer. Sci Rep 8: 2073, 2018.
41. Liu H, Yang M, Zhang Y, Yang Z, Chen Z, Xie Y, Peng B and Cai L: The effect of miR-539 regulating TRIAP1 on the apoptosis, proliferation, migration and invasion of osteosarcoma cells. Cancer Cell Int 21: 227, 2021.
42. Wong MM, Aziz NA, Ch'ng ES, Armon S, Chook JB, Bong JJ, Peh SC, Wu YS and Teow SY: Expression of LC3A, LC3B and p62/SQSTM1 autophagy proteins in hepatocellular carcinoma (HCC) tissues and the predicted microRNAs involved in the autophagy-related pathway. J Mol Histol 55: 317-328, 2024.
43. Yang Y, Lin Z, Han Z, Wu Z, Hua J, Zhong R, Zhao R, Ran H, Qu K, Huang H, *et al*: miR-539 activates the SAPK/JNK signaling pathway to promote ferropotosis in colorectal cancer by directly targeting TIPE. Cell Death Discov 7: 272, 2021.
44. Zhao J, Xu J and Zhang R: MicroRNA-539 inhibits colorectal cancer progression by directly targeting SOX4. Oncol Lett 16: 2693-2700, 2018.
45. Sánchez-Tilló E, de Barrios O, Siles L, Cuatrecasas M, Castells A and Postigo A: β-catenin/TCF4 complex induces the epithelial-to-mesenchymal transition (EMT)-activator ZEB1 to regulate tumor invasiveness. Proc Natl Acad Sci USA 108: 19204-19209, 2011.
46. Cortez MA, Ivan C, Valdecanas D, Wang X, Peltier HJ, Ye Y, Araujo L, Carbone DP, Shilo K, Giri DK, *et al*: PDL1 regulation by p53 via miR-34. J Natl Cancer Inst 108: djv303, 2015.

Copyright © 2026 Zhang et al. This work is licensed under a Creative Commons Attribution-NonCommercial-NoDerivatives 4.0 International (CC BY-NC-ND 4.0) License.